

Holographic read - write projector of video images

D. G. Papazoglou, M. Loulakis, G. Siganakakis and N. A. Vainos*

Foundation for Research and Technology-Hellas (FORTH), Institute of Electronic Structure & Laser, P.O. Box 1527,
Tel. +30 810 391273, Fax +30 810 391305, Vassilika Vouton, Heraklion 711 10, Crete, Greece
dpapa@iesl.forth.gr

* Present address: Engineered Photonic Media Lab, NHRF- National Hellenic Research Foundation, Theoretical and
Physical Chemistry Institute-TPCI 48, Vas. Constantinou Ave., Tel. +30 1 7273887, Athens 11635, Greece
vainos@eie.gr

Abstract: We demonstrate two real-time, read-write holographic projectors of video images based on photorefractive materials. A photorefractive crystal holographically records multiple, angularly multiplexed 2D images. By sequentially reconstructing each pre-recorded image a holographic video is created. In first setup the 2D image of an LCD screen is holographically recorded in a photorefractive LiNbO₃ crystal. In the second setup the Fourier transform of the LCD screen is recorded in the crystal. A detailed comparison of the two setups along with a number of videos is provided. The Fourier transform recording is superior in image quality compared to the direct image recording.

© 2002 Optical Society of America

OCIS codes: (160.5320) Photorefractive materials, (210.2860) Holographic and volume memories, (110.0110) Imaging systems, (110.4190) Multiple imaging, (110.6880) Three-dimensional image acquisition, (090.4220) Multiplex holography.

References and links

1. W. J. Hannan, R. E. Flory, M. Lurie, Ryan, "Holotape: A low-cost prerecorded television system using holographic storage," *J. Soc. Motion Pic. and Television Eng.*, **82**, 905 (1973)
2. H. B. Brown, "Holographic television techniques," *SPIE, Pract. Electro-Opt. Instr. Techn.*, **255**, 151 (1980)
3. G. Zhou, D. Psaltis and F. Mok, "Holographic read-only memory," *Opt. Quant. Elect.*, **32**, 405 (2000)
4. D. Psaltis, D. Brady and K. Wagner, "Adaptive optical networks using photorefractive crystals," *Appl. Opt.*, **27**, 1752 (1988)
5. H. Sasaki, N. Mauduit, J. Ma, Y. Fainman, S. H. Lee and M. S. Gray, "Dynamic digital photorefractive memory for optoelectronic neural network learning modules," *Appl. Opt.*, **35**, 4641, (1996)
6. N. J. Cook, A. Carnicer, S. Vallmitjana, I. Juvells, C. M. Cartwright, and W. A. Gillespie, "Implementation of a photorefractive binary joint transform correlator," *J. Opt. Soc. Am. B*, **15**, 1977 (1998)
7. A.D. Jacobson, V Evtuhov, J. K. Neeland, "Motion picture holography," *App. Phys. Lett.*, **14**, 120 (1969)
8. M. E. Cox, R.G. Buckles, D. Whitlow, "Cineholomicroscopy of small animal microcirculation," *App. Opt.*, **10**, 128 (1971)
9. E. N. Leith, D.B. Brumm, St. S. H. Hsiao, "Holographic Cinematography," *App. Opt.*, **11**, 2016 (1972)
10. P. Smigielski, H. Fagot, F. Albe, "Holographic cinematography with the help of a pulse YAG laser," *SPIE High Speed Phot.*, **491**, 750, (1984)
11. P. Smigielski, "Holographic cinematography and its applications," *SPIE Indust. Laser Interf.*, **746**, 29 (1987)
12. S. H. Lin, M. L. Hsieh, K. Y. Hsu, T. C. Hsieh, S. P. Lin, T. S. Yeh, L. J. Hu, C. H. Lin and H. Chang, "Photorefractive Fe:LiNbO₃ crystal thin plates for optical information processing," *J. Opt. Soc. Am. B*, **16**, 1112 (1999).
13. M. A. Neifeld, M. McDonald, "Optical design for page access to volume optical media," *Appl. Opt.*, **35**, 2418 (1996)
14. Q. Gao and R. Kostuk, "Cross-talk noise and storage capacity of holographic memories with a LiNbO₃ crystal in the open-circuit condition," *Appl. Opt.*, **37**, 929 (1998)
15. H. Rajbenbach, S. Bann, J. P. Huignard, "Long-term readout of photorefractive memories by using a storage/amplification two-crystal configuration," *Opt. Lett.*, **17**, 1712 (1992)

16. I. McMichael, W. Christian, D. Pletcher, T. Y. Chang, J. H. Hong, "Compact holographic storage demonstrator with rapid access," *App. Opt.*, **35**, 2375, (1996)
 17. J. Ma, T. Chang, S. Choi and J. Hong, "Ruggedized digital holographic data storage with fast access," *Opt. Quant. Elect.* **32**, 383, (2000)
 18. I. Zergioti, S. Mailis, N. A. Vainos, P. Papakonstantinou, C. Kalpouzos, C. P. Grigoropoulos, and C. Fotakis "Microdeposition of metal and oxide structures using ultrashort laser pulses," *Appl. Phys. A: Mater. Sci. Process.* **66**, 579 (1998)
-

1. Introduction

During the last 30 years many researchers have tried to exploit the benefits of holography in the fields of optical information storage and processing. In all the applications the recording media vary from the classical halide film to the dynamic photorefractive crystals [1-3]. The ability of the photorefractive crystals (PRC) to serve as holographic recording media for real time optical information processing gives new exciting capabilities [4-6] to somehow saturated fields of research.

An application of holography in 3D image recording and reconstruction is holographic cinematography [7-11]. The early attempts in holographic cinematography were successful in the laboratory but experienced technical difficulties in the real field. Holographic cinematography is actually a direct expansion of classic cinematography since the low-resolution film is replaced by a high resolution holographic one, and the camera by a holographic setup.

On the other hand the photorefractive crystals have been extensively used as holographic memories of 2D pages of data [12-15]. The use of error correction algorithms for the digital data pages recorded in the PRCs has lead to very low error rates [16, 17]. Any setup based on photorefractive crystals capable of storing a number of 2D pages of data can be used to store video frames. In this case each video frame would correspond to one page of data. If the holographic memory can be sequentially accessed in video frame rate (~25Hz) then the sequential reconstruction of the stored 2D pages would result in a holographic video. A holographic projector of video images is a holographic memory optimized for naked eye observation.

In the work presented here our goal is to demonstrate two holographic projector setups optimized for video sequence storage and reconstruction. Both the setups are capable of auto rewind (the first frame is reconstructed after the last) and continuous playing. This makes them perfectly suited for the storage of cyclic video sequences. The main difference between the two setups is the optical information recorded in the volume of the PRC. In the first setup the image of a Spatial Light Modulator (SLM) is holographically recorded in a rather straightforward way. In the second setup the Fourier transform of the SLM image is holographically recorded in the volume of the PRC.

2. Experimental setup

Both experimental setups are based on an iron doped $\text{LiNbO}_3\text{:Fe}$ photorefractive crystal and are presented in Figures 1a, 1b. The crystal is used as a real time read-write holographic medium. A 2D digital image of each video frame is transferred electronically from a PC to the SLM (LCD screen, 320x240 pixels resolution). During recording, each frame of the holographic video is recorded separately. No fixing of the holographically recorded images is preformed, therefore the recorded information are erased after continuous reading.

In the setup presented in figure 1a the SLM is illuminated through a diffuser (D) by an expanded laser beam (532nm Nd:YVO₄ laser) and then optically imaged by the photographic lens L₅ in the photorefractive crystal. The image size is approximately 1mm in diameter. Holographic recording takes place by the use of one of the 8 collimated reference beams.

Each reference beam corresponds to one 2D image and consequently to one frame of

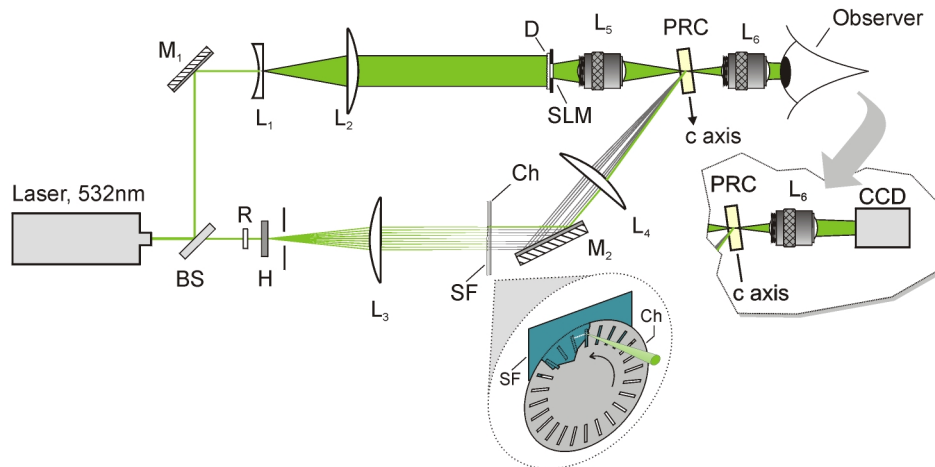


Fig. 1a. Direct image recording experimental setup. M_1 , M_2 Mirrors, BS variable beamsplitter, R $\lambda/2$ retardation plate, H Computer Generated Hologram (CGH), L_1 - L_4 lenses, (f_{L1} =100mm, f_{L2} =250mm, f_{L3} =200mm, f_{L4} =250mm), D diffuser, L_5 photographic lens f =50mm, L_6 phot. lens f =28mm, SF 8-pinhole spatial filter, Ch chopper, PRC photorefractive crystal $\text{LiNbO}_3\text{:Fe}$. The object and reference beams are extraordinary polarized. The image can be projected to a CCD detector by properly adjusting lens L_6 . The inset shows a magnified 3D view of the combination of the 8-pinhole spatial filter and the chopper.

one holographic video. The nominal angle between the object and the reference beams is 50° . The intensity ratio of the object beam to the reference beam is 4%. The reference beams are produced by the use of a specially designed Computer Generated Hologram (CGH) microetched on photoresist using ultra-fast pulsed UV laser microetching [18]. The CGH splits the laser beam into 8 angularly separated beams of equal intensity. A 4f system combined with an 8 pinhole spatial filter and a chopper provides the means of proper selection of the reference beams. The selection of a reference beam is preformed by the rotation of the chopper. Due to the symmetry of the 4f system the collimated reference beams are angularly but not spatially separated in the PRC where holographic recording takes place.

Since a volume phase hologram is recorded in the PRC the Bragg conditions apply,

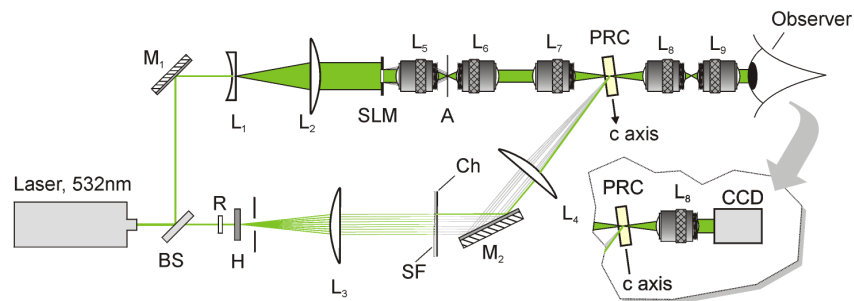


Fig. 1b. Fourier transform recording setup. M_1 , M_2 Mirrors, BS variable beamsplitter, R $\lambda/2$ retardation plate, H Computer Generated Hologram (CGH), L_1 - L_4 lenses, (f_{L1} =100mm, f_{L2} =250mm, f_{L3} =200mm, f_{L4} =250mm), L_5 photographic lens f =50mm, L_6 photographic lens f =58mm, L_7 phot. lens f =78mm, L_8 phot. lens f =58mm, L_9 phot. lens f =28mm, SF 8 pinhole spatial filter, Ch chopper, PRC photorefractive crystal $\text{LiNbO}_3\text{:Fe}$. The object and reference beams are extraordinary polarized.

therefore each image is reconstructed only by the use of the corresponding reference beam. By rotating the chopper, each of the reference beams illuminates the crystal resulting in the reconstruction of the corresponding image. The average diffraction efficiency of the reconstructed images is 0.045%. The sequential reconstruction of the images creates a holographic video. Furthermore, the cyclic repetition of the reference beams by the rotating chopper results in "auto-rewinding" of our video since the last frame is followed by the first one etc. The setup is capable of reconstructing in high frame rates (up to 4kHz) and this is determined only by the maximum rotational speed of the chopper. The reconstructed image is viewed by the use of the photographic lens L_6 . The reconstructed video sequence can be also projected on a CCD camera detector by properly adjusting lens L_6 .

In the setup presented in Fig 1b an expanded laser beam illuminates the SLM. The SLM image is Fourier transformed by photographic lens L_5 . Since the SLM is pixelated the Fourier transform of the image is repeated over several orders. A rectangular aperture (A) located on the Fourier plane of lens L_5 filters out the higher components except the zero order. A 4f system composed by photographic lenses L_6 , L_7 is used to image the filtered Fourier transform in the volume of the crystal. The image size is again ~ 1 mm in diameter. The part of the setup that corresponds to the production of the collimated reference beams is exactly the same as in the previous setup. The nominal angle between the object and the reference beams is 50° . The intensity ratio of the object to reference is 1.1%.

Again the corresponding image is reconstructed by rotating the chopper so that each of the reference beams illuminates the crystal. The average diffraction efficiency of the reconstructed images is 0.16%. The reconstructed video sequence is observed by the use of an x2 telescopic system consisted of lenses L_8 , L_9 . The magnification of this system is approximately x2. A similar telescope system was constructed by using simple plano-convex lenses with a small drop in image quality. The image can be also projected on a CCD camera detector by simply using lens L_8 .

An overall of ten sample videos are presented here. All of them were specially designed so that a continuous flow of images is observed after each auto rewind. A CCD detector and a



Fig. 2a. (935 Kb) Video presenting a rotating 2D propeller recorded in the direct image recording setup (Figure 1a).

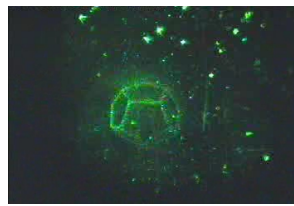


Fig. 2c. (825 Kb) Video presenting a rotating 3D dodecahedron recorded in the direct image recording setup (Figure 1a).

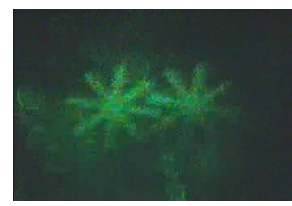


Fig. 2e. (844 Kb) Video presenting a set of two rotating 2D gears recorded in the direct image recording setup (Figure 1a).

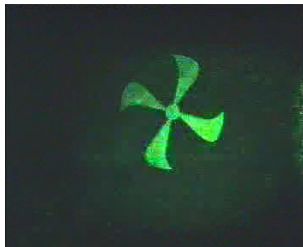


Fig. 2b. (862 Kb) Video presenting a rotating 2D propeller recorded in the Fourier transform recording setup (Figure 1b).

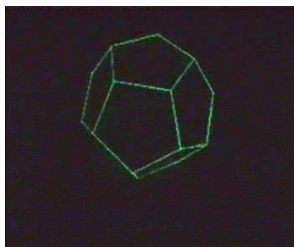


Fig. 2d. (706 Kb) Video presenting a rotating 3D dodecahedron recorded in the Fourier transform recording setup (Figure 1b).



Fig. 2f. (943 Kb) Video presenting a set of two rotating 2D gears recorded in the Fourier transform recording setup (Figure 1b).



Figure 3. (1.74 Mb) Video presenting a rotating 2D propeller recorded in the Fourier transform recording setup (Figure 1b). The reconstruction speed is variable so stroboscopic effects are observed.

video grabber were used to capture them (figure 1a, figure 1b) and they approximate the visual effect experienced by a naked eye observer. The first six videos are grouped in pairs and are used to compare the recording and reconstruction quality between the presented setups. In all three pairs the same video sequence is recorded in the setup presented in figure 1a and in the setup presented in figure 1b. Specifically figure 2a, figure 2b represent a simple rotating 2D propeller. Figure 2c, figure 2d represent a rotating 3D dodecahedron. Finally, figure 2e, figure 2f represent a set of two rotating 2D gears.

Figures 2a, 2c, 2e were recorded and reconstructed by the use of the experimental setup presented in figure 1a, while figures 2b, 2d, 2f were recorded and reconstructed by the use of the experimental setup presented in figure 1b.

It is clear from all the videos that the setup presented in figure 1b produces video sequences of higher resolution. The main reason for this is that no diffuser is used. Furthermore, the recorded image is viewed at infinity and not in the crystal volume as in the simpler setup presented in figure 1a. This effectively reduces the optical noise produced by imperfections in the crystal.

Four more video sequences are presented here. They are all recorded and reconstructed by the use of the setup presented in figure 1b. Figure 3 is actually the same rotating 2D propeller presented in figure 2b. The only difference in this video is that the reconstruction speed varies, slowing down from approximately 50Hz to 4Hz. Due to this a stroboscopic effect can be viewed.

Figure 4a presents various views of a rotating stellated dodecahedron while figure 4b presents a rotating complex structure. Finally, figure 4c presents a rotating 3D lobe.

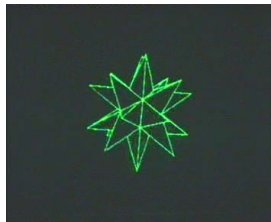


Figure 4a. (1 Mb) Video presenting a rotating 3D stellated dodecahedron recorded in the Fourier transform recording setup (Figure 1b).

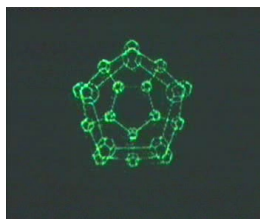


Figure 4b. (1 Mb) Video presenting a rotating 3D complex structure recorded in the Fourier transform recording setup (Figure 1b).

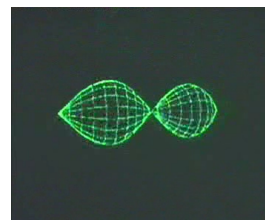


Figure 4c. (485 Kb) Video presenting a rotating 3D lobe recorded in the Fourier transform recording setup (Figure 1b).

3. Conclusions-Discussion

The capability of photorefractive crystals to record and read optical information in real time makes it possible to expand their use as active optical components. We have demonstrated that by fast addressing in real time an angularly multiplexed holographic projector one can

view a continuous video flow. Since image quality is of major concern in all projector systems the holographic recording of the Fourier transform instead of the SLM image in the volume of the PRC is the optimum solution. The only drawback in this technique is the need for use of more complicated optics.

The maximum number of reference beams and consequently of available frames is determined by the Bragg conditions. Typical values of the angular selectivity due to the Bragg conditions for a few millimeter-sized PRC crystals are in the order of 1.5×10^{-4} deg [14]. A practical limit for angular multiplexing of thick phase gratings in PRC crystals is ~1200 frames [16].

The projection technique can be expanded so that a series of stereoscopic, angularly separated 2D views of a 3D graphical object are recorded in each frame. This will result in an auto-stereoscopic 3D video.